Evidence for the Role of Ions in Aerosol Nucleation

Martin B. Enghoff,*,† Jens Olaf Pepke Pedersen,† Torsten Bondo,† Matthew S. Johnson,‡ Sean Paling,§ and Henrik Svensmark†

Center for Sun-Climate Research, National Space Institute, Technical University of Denmark, DK-2100 Copenhagen, Denmark; Copenhagen Center for Atmospheric Research, Department of Chemistry, University of Copenhagen, DK-2100 Copenhagen, Denmark; and Department of Physics and Astronomy, Sheffield University, Sheffield S10 2TN, U.K.

Received: April 25, 2008

Aerosol nucleation has been studied experimentally in purified, atmospheric air, containing trace amounts of water vapor, ozone, and sulfur dioxide. The results are compared with model calculations. It is found that an increase in ionization by a factor of 10 increases the production rate of stable clusters by a factor of ~3, probably due to ion-induced nucleation.

1. Introduction

The role of ions in producing aerosols in the earth's atmosphere is a very active area of research. Atmospheric[1−5] and experimental[6] observations have shown that the nucleation of aerosol particles can occur under conditions that cannot be explained by classical nucleation theory. Several ideas have been put forward to solve this nucleation problem, e.g., ion-induced nucleation[7−9] and ternary nucleation.[5] However, experimental investigations exploring the role of ions in particle production are scarce and often in conditions far removed from those relevant for the lower part of the atmosphere.[10−14]

Recently, experimental work[15] demonstrated that ions, produced by cosmic rays in the atmosphere, are likely to play an important role in the production of new aerosol particles. The mechanism whereby energetic cosmic rays can promote the production of cloud condensation nuclei at low altitudes constitutes a link between cosmic rays and the earth's climate, and there is thus a need to corroborate the results in a different experiment. The present results, which are obtained in the same laboratory, but using a new setup with a much smaller (50 L) reaction chamber, confirm the previous conclusions, which were obtained with a 7 m^3 reaction chamber.

2. Experimental Methods

The present experiments were conducted in a cylindrical reaction chamber (length 100 cm and diameter 25 cm) made of electropolished stainless steel. One end of the chamber consists of a thin Teflon foil to allow transmittance of UV light. The chamber was continuously flushed with air at a rate of 3.2−3.3 L/min to maintain steady-state conditions and allow for mixing. The air consisted of atmospheric air, compressed and dried with an oil-free compressor and filtered using active charcoal, citric acid, and 10 nm as well as 3 nm filters. A mixture of ozone, SO_2, and water vapor was added to the air flow before entering the chamber. The air entered through a tube protuding about 80 cm into the chamber from the opposite end of the Teflon window, and sampling also took place at the tube-insertion end.

The air was humidified by circulating deionized water through a GoreTex tube inserted into the air stream. This allowed the relative humidities to be varied from 5 to 90%. Sulfur dioxide was added to the chamber from a 5 ppm mixture of SO_2 in dry air (Strandmøllen), and ozone was introduced by flowing air through an ozone generator. SO_2 and O_3 flowed through a separate tube with a 3 nm particle filter and was joined with the main air flow at the very entrance to the chamber.

The pressure in the chamber was held at 1 mbar above atmospheric pressure, and the temperature was that of the room, which was temperature stabilized.

A mercury discharge lamp placed about 135 cm from the Teflon window emitted UV radiation primarily at 253.7 nm, which was collimated by a black, 80 mm, $^1/_4$ in. pore size honeycomb wall. This initiated a photochemical reaction where ozone was photolyzed to produce OH radicals, and by reaction with sulfur dioxide and subsequently with oxygen and water, sulfuric acid was produced to begin nucleation. The participation of trace amounts of other compounds (which may not be trapped by the filters) in the nucleation process can, however, not be ruled out.

Temperature, pressure, and relative humidity were monitored as well as ozone and sulfur dioxide concentrations using trace gas analyzers at the 0.1 ppb (Teledyne model 400A) and 0.05 ppb (Thermo model 43 CTL) level, respectively.

Ions in the chamber were produced by cosmic radiation and the decay of the natural abundance of radon. In addition to this, the production of ion pairs could be increased by a 35 MBq Cs-137 gamma source. This source was placed at the long side of the chamber, ~140 cm from the center. The resulting ionization was measured by a Gerdien tube[16] and varied from 770 ion pairs/cm^3 without the gamma source to 3700 ion pairs/cm^3 with the source fully open. The strength of the source could be varied by placing pieces of lead in front of the source. For this experiment we either had the source fully open, fully closed (10 cm of lead), or covered by 1 cm of lead (corresponding to approximately a 50% reduction). From the measured ion densities and other known parameters for the chamber the ion pair production from cosmic radiation and radon is estimated to about 3.7 cm^{-3} s^{-1}. With the gamma source this number increases to about 35 cm^{-3} s^{-1}.

The resulting aerosol production was measured by a TSI Ultra Fine Condensation Particle Counter model 3025A.

* To whom correspondence should be addressed.
† Technical University of Denmark.
‡ University of Copenhagen.
§ Sheffield University.

10.1021/jp806852d CCC: $40.75
Published on Web 09/12/2008

The previous experiments were conducted in a 7 m^3 reaction chamber made of Mylar and Teflon. Inside the chamber two 1.7×1.7 m^2 electrodes were placed to allow for the generation of an electric field, meant to remove ions. External UV lamps were used to initiate the photochemistry in the chamber in a way similar to that described for the present setup. Further details can be found in the paper describing the experiment.[15]

The experiments described in this paper were conducted by allowing SO_2, O_3, the temperature (T), and the relative humidity (RH) to settle into a steady state in the chamber. Prior to the measurements, the chamber was cleansed using UV and ozone for 1 week, followed by 6 days of conditioning before the measurements became reproducible. Typically T was held around 23 °C and RH at 50%. Two series of measurements were performed: the first one (I) with SO_2 set to 4 ppb and O_3 to 23 ppb and a second series (II) with SO_2 set to 30 ppb and O_3 to 68 ppb. Atmospheric levels of SO_2 range from ~20 ppt in the marine surface layer to ~1.5 ppb in polluted areas, and O_3 concentrations lie between 20 and >200 ppb. Whereas our O_3 values are within the range of the atmosphere, our lowest SO_2 values (series I) are somewhat above atmospheric levels. However, with the current setup lower concentrations of SO_2 would lead to particle concentrations below the detection level of the particle counter.

In both series a measurement was initiated with the production of a "burst" of H_2SO_4 following exposure of the chamber to UV light, resulting in the production of aerosols. The peak aerosol concentration lasted for a few minutes before decaying exponentially due to wall and dilution losses. Figure 1 shows a typical measurement of the particles by the condensation particle counter, which measures particles larger than ~3 nm. An initial steep rise in aerosol number to a maximum is followed by a slower decay. The small size of the reaction chamber allowed for a return to initial conditions after about 1.5 h, and the cycle could be repeated with another burst of UV light. In series I the chamber was illuminated for 11 min with 110 min between each measurement, and in series II there was 4 min of exposure to UV at 10 times lower intensity than in series I with 90 min between each measurement.

As a measure of the number of particles produced we integrate the peak over time by adding count numbers from each individual measurement. The results from the two continuous measurement series can be seen in Figure 2, where the integrated peak values are shown as a function of time. During each series the ion density in the reaction chamber was varied by changing the intensity of the Cs-137 source as described above.

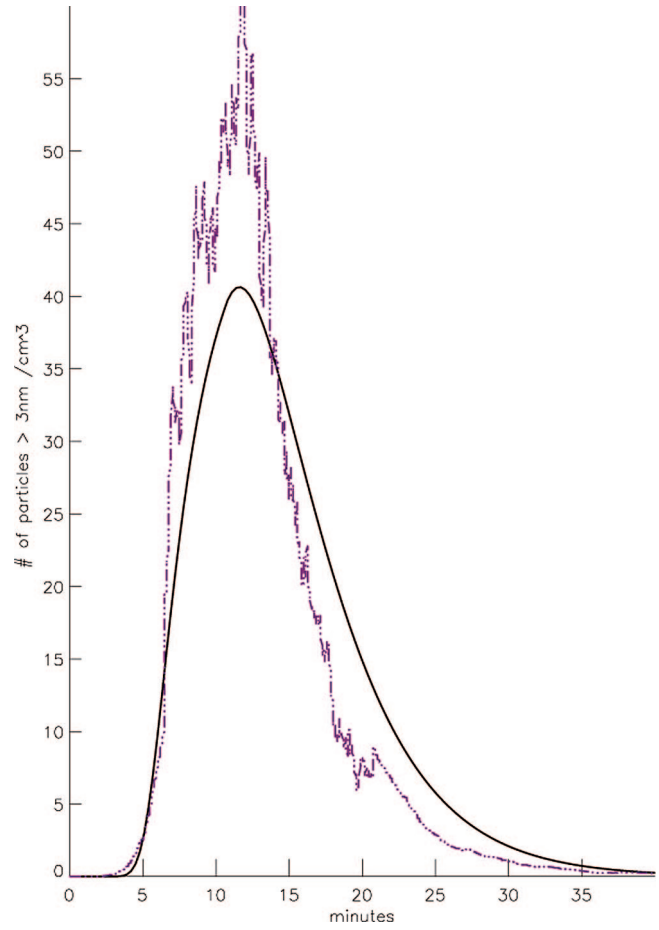

Figure 1. Example of measurement of the particles by the condensation particle counter (dashed line). Time is measured after start of the UV illumination. Only particles larger than ~3 nm are detected by the particle counter. The solid line is the result of a model that generates the same number of particles (see text).

3. Results and Discussion

It is seen from Figure 2 that there is clear dependency of the number of particles on the level of radiation. For series I the mean value of the integrated peak is ~19 600 with no exposure to the gamma source and ~53 600 with full exposure. For series II the value is ~5800, ~11 300, and ~19 500 for no exposure, 1 cm of lead in front of the source, and full exposure, respectively.

A numerical model of neutral sulfuric acid particle growth has been developed to aid the interpretation of the experimental results and to examine the dependence of the particle production at 3 nm to changes in the sulfuric acid gas concentration and particle nucleation rates.

The model is based on the general dynamic equation (GDE) which is a partial differential equation for aerosol particle growth [ref 17, Chapter 12]. A sectional method is used to solve the GDE to determine the number distribution n. Separate bins represent different sizes of the molecular clusters expressed as the number of sulfuric acid molecules in the cluster. The size of the cluster in a given bin increases stepwise by 1 molecule up to 70 molecules (~3.5 nm cluster diameter), where the cluster size is then increased by larger steps, as shown in eq 1. With i being the bin number, $nc(i)$ the size of the cluster in bin i, and $nmax$ a factor used to determine the largest cluster described in the model, the cluster sizes are defined by

$$nc(i) = [0, 1, 2, ..., 69, 70, 75, 85, 100, 120, 145, 175, 210, 250, 250 \times 1.2^{j+1}], \quad j \in [0, nmax] \quad (1)$$

Adopting equivalent notation to that of Lovejoy et al.,[18] the discrete partial derivative of the neutral sulfuric acid cluster distribution function for bin i, $n(i)$, is now given by

$$\frac{\partial n(i)}{\partial t} = \frac{k^c_{i-1}[H_2SO_4]n(i-1)}{(nc_i - nc_{i-2})/2} - \frac{k^c_i[H_2SO_4]n(i)}{(nc_{i+1} - nc_{i-1})/2} + 0.5\sum_l \sum_j k^e_{j,l} n(j)n(l) \frac{(nc_l + nc_j) - nc_{i-1}}{(nc_i - nc_{i-1})} \delta_{(n_l+n_j),[nc_{i-1},nc_i]} + 0.5\sum_l \sum_j k^e_{j,l} n(j)n(l) \frac{nc_{i+1} - (nc_l + nc_j)}{(nc_{i+1} - nc_i)} \delta_{(n_l+n_j),[nc_{i+1},nc_i]} - \lambda_{par} n(i) \quad (2)$$

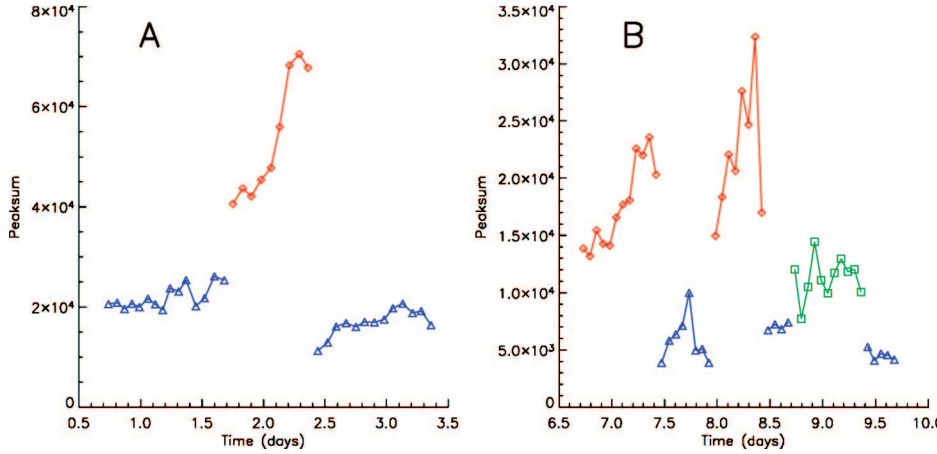

Figure 2. Results from the two measurements series—the integrated peak is shown as a function of time. Blue triangles correspond to measurements without the gamma source (ion production ~3.7 cm^{-3} s^{-1}), red diamonds are with the source open (ion production ~35 cm^{-3} s^{-1}), and green squares are with 1 cm of lead in front of the source (intermediate ion production). RH was ~50% and $T \sim 23$ °C for both series. (A) ~4 ppb SO_2 and ~23 ppb O_3 with 11 min of UV and 110 min between each measurement. (B) ~30 ppb SO_2 and ~68 ppb O_3 with 4 min of exposure to UV at 10 times lower intensity than in the first series and 90 min between each measurement.

The first term is the production of $n(i)$ from the previous bin by the condensation of a sulfuric acid molecule. The second term is similarly the loss due to condensation. The next two terms represent the coagulation of the individual clusters. Here the delta functions and the fractions take the increasing sizes of the bins into account and make sure to fractionalize the coagulated particles into the correct bins. The last term is a loss term used to account for losses of particles to the wall. Notice that evaporation is not considered since the particles are considered to be stable.

The condensation coefficients k_i^c are found according to Laakso et al.[19] with a value of the mass accommodation coefficient of 1,[20] where the mean free paths used to determine k_i^c are determined from Lehtinen et al.[21] The cluster diameter as a function of bin size must also be found. This is nontrivial since the mole fraction of water in the cluster changes with cluster growth. Here it is assumed that an initial sulfuric acid particle is wet, and the results from Seinfeld and Pandis [ref 17, p 486] are used to determine the cluster diameter and mole fraction of water as a function of number of sulfuric acid molecules. Having determined the particle diameter, the individual diffusion coefficients used in k_i^c are given by Poling et al.[22]

The coagulation coefficients are determined from Laakso et al.[19] and can be used in all growth regimes from diameters of a few angstroms to sizes larger than 1 μm. The model does not go into the chemistry of the nucleation but assumes that stable clusters with a size of five sulfuric acid molecules are formed at a rate s.

In each time step the sulfuric acid concentration is found by solving the rate equation

$$\frac{d[H_2SO_4]}{dt} = P_{H_2SO_4} - \lambda_{gas}[H_2SO_4] - [H_2SO_4]\sum_i n_i k_i^c \quad (3)$$

The first term, $P_{H_2SO_4}$, is the production term of sulfuric acid in cm^{-3} s^{-1}, and the second term is a loss term used to account for losses of gas molecules to the wall and dilution (λ_{gas} is the loss rate). The last term represents the loss of gas molecules due to condensation unto clusters, where n_i is the cluster concentration.

The model is initally run with a constant stable cluster production s, meaning that particles are being put into bin 5 at a constant rate. This ensures that steady-state conditions are obtained before turning on the sulfuric gas production $P_{H_2SO_4}$. The experimental data in series I and II are then modeled by turning on the production rate of sulfuric acid $P_{H_2SO_4}$ (for 11 and 4 min, respectively). An example is shown in Figure 1, where the model curve has been fitted to the experimental data for a set value of s and $P_{H_2SO_4}$.

The values of $P_{H_2SO_4}$ will lead to different sulfuric acid gas concentrations. By running the model, it was observed that the sulfuric acid gas concentration is independent of s for the range of values used. This means that the peak sulfuric acid concentration obtained for a particular production rate is also independent of s.

The sulfuric acid and particle losses (to walls and dilution) are set to 3.26 min for series I and 2.71 min for series II (determined experimentally from the decay of the aerosol peaks). The relative humidity was fixed at 50% for both series.

The output of each model run is a time series of the particle population adjusted for the counting effiency of the particle counter. Unique values, comparable with the experimental results, are obtained for each set of parameters by integrating the peaks over time.

For series I the model was run with equidistant ds = 0.05 cm^{-3} s^{-1} with s = [0.05, 7.35] cm^{-3} s^{-1} and equidistant d$P_{H_2SO_4}$ = 45 000 cm^{-3} s^{-1} with $P_{H_2SO_4}$ = [6.5 × 10^4, 2 × 10^6] cm^{-3} s^{-1}. For series II ds = 0.05 cm^{-3} s^{-1} with s = [0.05, 5] cm^{-3} s^{-1} and d$P_{H_2SO_4}$ = 90 000 cm^{-3} s^{-1} with $P_{H_2SO_4}$ = [4 × 10^4, 4 × 10^6] cm^{-3} s^{-1}.

Figure 3 shows these values for the two series I (left) and II (right).

The insets in Figure 3 show model results compared to experimental data for selected values of s and peak sulfuric acid gas concentrations and thus show the effect on the experimental signal of changes in these two parameters. The model fits the experimental data in series I rather well, whereas the actual shape of the model results in series II differs more from the shape of the experimentally obtained peaks. A more detailed model including evaporation might improve this. However, for the purpose of determining approximate values of particle and gas concentrations the model is sufficient.

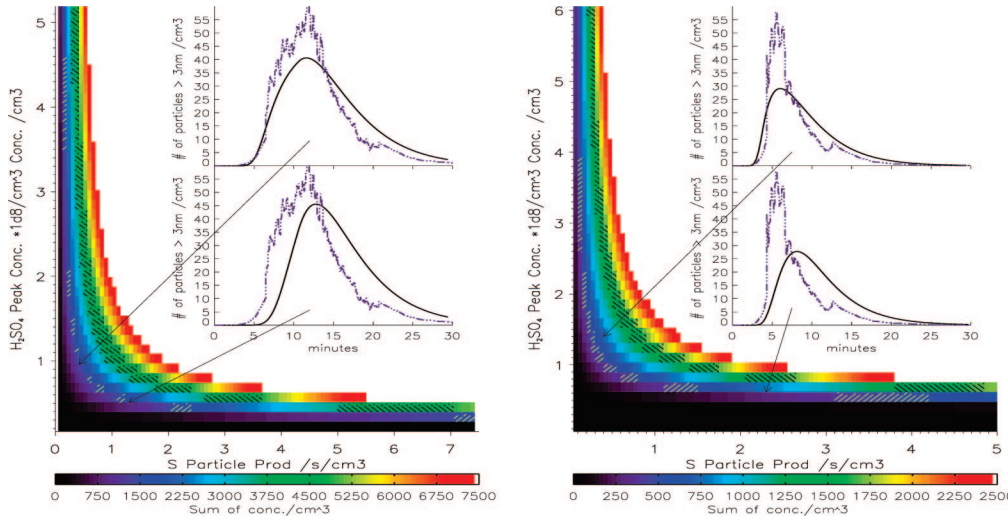

Figure 3. Integrated value of the temporal evolution of the formation of aerosols adjusted for the counting effiency of the particle counter as a function of *s* and sulfuric acid concentration. Left: series I. Right: series II. Hatched with / are the experimental data without sources, and hatched with \ are the experimental data with fully open sources. The experimental data used in this figure are obtained by computing the average of the values in Figure 2 with and without sources and including the 95% confidence interval. The insets shows model results compared to experimental data for selected values of *s* and peak sulfuric acid gas concentrations.

The results show that the number of generated aerosols depend on the level of exposure to the gamma sources—the question is what mechanism controls this. A concern when using γ radiation to ionize the gas is that this may produce additional sulfuric acid directly by radiolysis of water (leading to OH, which reacts with SO_2 and forms H_2SO_4). We can exclude this possibility by looking at the time it takes from when the UV light is turned on in the experiment until the aerosol concentration exceeds a certain level, which we have chosen to be 5 cm^{-3}. An increase in sulfuric acid would cause a faster growth of the particles and thus shorter delay time. In general, this delay time is seen to be reduced when the gamma source is open; however, since there is 7 times more SO_2 in the series II experiment compared to the series I, it would be expected that the relative increase of H_2SO_4 and therefore delay time would be much larger in series II compared to series I. Looking at the relative increase it is, however, 1.31 for series I and 1.35 for series II, i.e., almost identical changes. We thus take this to prove that the observed increase in aerosol production with increased ionization is not due to an increase in sulfuric acid from radiolysis. The delay time and the general shape of the model solution can now be used to constrain the experimental values of *s* and the sulfuric acid concentration. For both series I and II we constrain the sulfuric acid concentration to the range of $C_{H_2SO_4} \approx (0.5-2.5) \times 10^8$ cm^{-3}. This concentration is well below the range where homogeneous nucleation is expected to dominate [ref 17, p 523, Figure 11.11].

Another possible explanation for the results is that the surface properties of the chamber change, such that the loss rate for the particles is reduced or gases are released from the walls. However, no significant change in the loss rate to the walls was observed when the chamber was exposed to the gamma source so this cannot be the explanation either, leaving ion-induced nucleation as the only viable explanation for the observations. For both series, at a given sulfuric acid concentration, an increase in stable cluster production by a factor of $\sim$3 is required to explain the difference between full and no exposure to the gamma source. In this experiment the ion production rate increases by a factor of 10 (from $\sim$4 to $\sim$40 cm^{-3} s^{-1}).

The previous experiments[15] showed a linear dependency of the amount of particles produced on the small ion density and gave an empirical relation between the measured ion concentration and the production rate of new clusters (*s*). According to this relationship ($s = 2.4 \times 10^{-4} n_e$, where n_e is the ion concentration), *s* should go from 0.19 cm^{-3} s^{-1} without exposure to the source to 0.89 cm^{-3} s^{-1} with full exposure. This is well within the limits given by the present results, when the constrained values for the sulfuric acid concentration is used to determine *s*. The increase in cluster production suggested by the previous study, from no to full exposure, is by a factor of 4.8, which is to be compared to the factor of $\sim$3 found in this paper.

4. Conclusions

In conclusion, the present experiment confirms the previous result that ions play a role in nucleating new aerosols in the atmosphere and that the rate of production is sensitive to the ion density. Most likely the aerosols produced in the experiment are formed by sulfuric acid and water, but the participation of other compounds, which may not be removed by the filters, cannot be excluded.

The presence of a penetrating cosmic ray background limits the minimum ionization for which aerosol production can be investigated in our laboratory. An experiment that can be performed under ultralow background radiation conditions is therefore in progress.

Acknowledgment. We thank Freddy Christiansen for help with developing the model.

References and Notes

(1) Hoppel, W. A.; Frick, G. M.; Fitzgerald, J.; Larson, R. E. *J. Geophys. Res.* **1994**, *99*, 443.

(2) Clarke, A. D.; Davis, D.; Kapustin, V. N.; Eisele, F.; Chen, G.; Paluch, I.; Lenschow, D.; Bandy, A. R.; Thornton, D.; Moore, K.; Mauldin, L.; Tanner, D.; Litchy, M.; Carroll, M. A.; Collins, J.; Albercook, G. *Science* **1998**, *282*, 89.

(3) Birmili, W.; Berresheim, H.; Plass-Dülmer, C.; Elste, T.; Gilge, S.; Wiedensohler, A.; Uhrner, U. *Atmos. Chem. Phys.* **2003**, *3*, 361.

(4) Lee, S.-H.; Reeves, J. M.; Wilson, J. C.; Hunton, D. E.; Viggiano, A. A.; Miller, T. M.; Ballenthin, J. O.; Lait, L. R. *Science* **2003**, *301*, 1886.

(5) Kulmala, M.; Pirjola, L.; Mäkelä, J. M. *Nature (London)* **2000**, *404*, 66.

(6) Berndt, T.; Böge, O.; Stratmann, F.; Heintzenberg, J.; Kulmala, M. *Science* **2005**, *307*, 698.

(7) Arnold, F. *Nature (London)* **1980**, *284*, 610.

(8) Raes, F.; Janssens, A.; van Dingenen, R. *J. Aerosol Sci.* **1986**, *17*, 466.

(9) Turco, R. P.; Zhao, J. X.; Yu, F. *Geophys. Res. Lett.* **1998**, *25*, 635.

(10) Bricard, J.; Billard, F.; Madelaine, G. *J. Geophys. Res.* **1968**, *73*, 4487.

(11) Vohra, K. G.; Ramu, M. C. S.; Muraleedharan, T. S. *Atmos. Environ.* **1984**, *18*, 1653.

(12) Nagato, K.; Kim, C. S.; Adachi, M.; Okuyama, K. *J. Aerosol Sci.* **2005**, *36*, 1036.

(13) Kim, C. S.; Adachi, M.; Okuyama, K.; Seinfeld, J. H. *Aerosol Sci. Technol.* **2002**, *36*, 941.

(14) Wilhelm, S.; Eichkorn, S.; Wiedner, D.; Pirjola, L.; Arnold, F. *Atmos. Environ.* **2003**, *38*, 1734.

(15) Svensmark, H.; Pedersen, J. O. P.; Marsh, N. D.; Enghoff, M. B.; Uggerhøj, U. I. *Proc. R. Soc. London A* **2007**, *463*, 385.

(16) Aplin, K. L.; Harrison, R. G. *Rev. Sci. Instrum.* **2000**, *71*, 3037.

(17) Seinfeld, J. H.; Pandis, S. N. In *Atmospheric Chemistry and Physics*, 2nd ed.; Wiley & Sons: New York, 2006.

(18) Lovejoy, E. R.; Curtius, J.; Froyd, K. D. *J. Geophys. Res.* **2004**, *109*, D08204.

(19) Laakso, L.; Mäkelä, J. M.; Pirjola, L.; Kulmala, M. *J. Geophys. Res.* **2002**, *107*, 4427.

(20) Laaksonen, A.; Vesala, T.; Kulmala, M.; Winkler, P. M.; Wagner, P. E. *Atmos. Chem. Phys.* **2005**, *5*, 461.

(21) Lehtinen, K. E. J.; Kulmala, M. *Atmos. Chem. Phys.* **2002**, *3*, 251.

(22) Poling, B. E.; Prausnitz, J. M.; O'Connell, J. P. In *Properties of Gases and Liquids*, 5th ed.; McGraw-Hill: New York, 2001.

JP806852D